

Article

Adsorptive removal and catalytic performance of metal-organic frameworks containing mixed azolium-bipyridine ligand

Nadia Gholampour¹, Chizoba I. Ezugwu^{1,2}, Shima Rahmdele³, Ali Ghanadzadeh Gilanie³, Francis Verpoort^{1,4,5*}

¹Laboratory of Organometallics, Catalysis and Ordered Materials, State Key Laboratory of Advanced Technology for Materials Synthesis and Processing, Wuhan University of Technology, Wuhan 430070, PR China.

²Department of Chemical Engineering, University of Alcalá, E-28871 Alcalá de Henares, Madrid, Spain.

³Department of Chemistry, Faculty of Science, University of Guilan, Rasht, Iran.

⁴National Research Tomsk Polytechnic University, Lenin Avenue 30, 634050 Tomsk, Russian Federation.

⁵Ghent University Global Campus, Songdo, 119 Songdomunhwa-Ro, Yeonsu-Gu, Incheon, Republic of Korea.

* Correspondence: francis.verpoort@ghent.ac.kr

Abstract: Two ligands, **1**, 3-bis(4-carboxyphenyl)imidazolium chloride and **4**, 4'-bipyridine, were employed to prepare nickel and zinc azolium based MOFs, **1** and **2** by the mixed ligand solvothermal approach. The positively charged azolium moieties in the imidazolium linker resulted in a charged environment in the as-synthesized frameworks. As a result, **1** and **2** demonstrated preferential adsorption of CO₂ over methane molecules in the gas phase adsorption due to the higher quadrupole moment of CO₂, which interacts more with the positively charged frameworks. Besides, in aqueous media, **1** and **2** exhibited incredible adsorption efficiency for anionic dyes. In the following, MOF **1** was metallated at the carbene site of the azolium linker to generate the novel heterogeneous catalyst **1-Pd**, which was successfully applied for Sonogashira and Suzuki-Miyaura coupling reactions without losing its activity after three cycles.

Keywords: Azolium MOFs; Dye adsorption; Post modification; Cross-coupling reactions

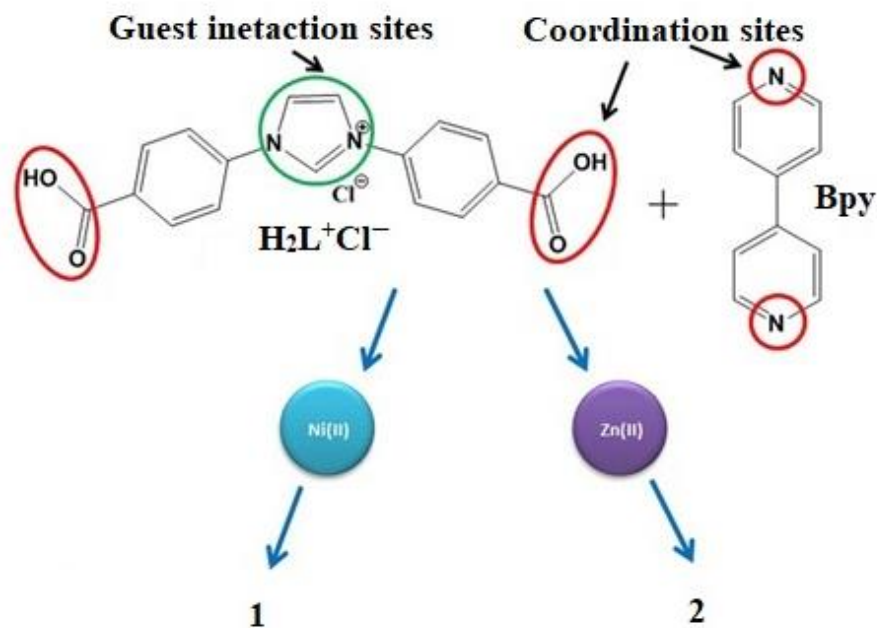
1. Introduction

Work over the last two decades on a class of materials known as metal organic frameworks (MOFs) or porous polymers (PCPs) has evolved to an unparalleled level of activity based on their high surface area[1], well-defined pore architectures[2], and tunable structural features[3]. MOFs gained much interest, not only because of their various applications but also because of their ability to be built by a linker with an extra active site that can be pre-, in-situ, or post-synthetically modified. An excellent example of such linkers is the azolium-containing ligands, precursors for N-heterocyclic carbenes (NHC). These imidazolium salt linkers are considered a novel strategy for creating electrostatic environments within the frameworks[4]. Therefore, these cationic components can increase the interaction between MOF and guest molecules. The proton conductivity of azolium linkers enhances their particular adsorption of gas molecules, including varying quadrupole moment and polarization. Azolium-containing MOFs show selective sorption of CO₂ over a non-polar gas

such as N_2 and CH_4 [4, 5]. Hence, gaseous molecules with higher quadrupole moment and polarizability preferentially would be adsorbed due to their remarkable interaction with the framework.

Nowadays, many synthetic organic dyes are consumed in various industries, such as the textile industry[6], leather tanning industry[7], paper production[8], and hair colorings[9]. Unfortunately, these organic dyes are a concern as they may give rise to significant non-aesthetic pollution and severe health problems[10]. Adsorption is considered a highly competitive technique attributed to its broad application scope, economic viability, and high performance, which is employed to reduce these synthetic dyes from the wastewater and environment[11]. Due to the inadequate absorptivity of traditional adsorbent like activated carbon[12], researchers have been looking for an advanced alternative. Regarding MOF's multiple properties, like high surface areas, large pore volume[13], pores surface functionalization, and host-guest interactions[14-16], make them a competitive candidate for this purpose. Ionic MOFs include more distinctive merits, such as selective adsorption of cationic or anionic dyes through host-guest electronic interactions, guest-guest exchange interactions, or both. Accordingly, azolium-based metal-organic frameworks may propel the adsorption properties since the charged azolium moieties interact with ionic organic substrates (like ionic dyes). Besides, the ionic substrates can be adsorbed and desorbed reversibly[17-19]. Interestingly, MOFs are considered as heterogeneous catalysts with both advantages of homogeneous and heterogeneous properties[20]. MOFs can provoke catalyzed reactions through the use of unsaturated metal coordination sites[21], fabrication of transition metal nanoparticles inside the pores[22], employing metal complexes chelated through the ligand as linker[23], and post-synthetic modification (PMS) (functionalization of the linker such as an azolium linker)[23, 24]. Sonogashira and Suzuki-Miyaura C-C coupling reactions are two well-known reactions in modern organic synthesis, usually catalyzed by palladium. The coupling products have been applied as intermediates to synthesize pharmaceuticals, natural products, biologically active molecules, and conjugated polymers[25, 26].

Up till now, there is still a knowledge gap in employing mixed azolium-pyridine based MOFs for the removal of charged organic pollutants from aqueous solutions. In this work, a mixed ligand solvothermal synthetic approach was successfully applied to prepare two azolium-pyridine based-MOFs, **1** and **2** (Scheme 1). MOF **1** and **2** were evaluated for the adsorptive removal of positively charged dye molecules from an aqueous medium, thereby establishing their potential application for wastewater treatment. Moreover, the as-synthesized frameworks proved highly efficient for the selective adsorption of CO_2 over non-quadrupole CH_4 . Also, the PSM of **1** with Pd resulted in forming a new heterogeneous NHC catalyst, **1**-Pd, which manifests as an efficient catalyst for Sonogashira and Suzuki-Miyaura C-C coupling reactions. This work may shed light on exploiting these hybrid framework materials to remove organic contaminants, gas separation, and catalysis.



Scheme. 1 Synthetic scheme of 1 and 2 applying mixed azolium-pyridine ligands.

2. Results

2.1. Characterization of compound 1 and 2

$H_2L^+Cl^-$ ligand was prepared in the lab, as Figure S1 demonstrates the 1H -NMR spectrum of $H_2L^+Cl^-$ agrees well with the literature[27].

Field emission scanning electron microscopy (FE-SEM) was applied to study the surface morphology of as-prepared MOFs. As illustrated in Figure 1, the FE-SEM images of 1(a) and 2(b) show a homogeneous surface morphology. The uniform microcrystals also indicate the high crystalline nature of the frameworks. The as-synthesized MOF, 1, reveals a uniform flower-like microcrystal with an average particle size of 1.3 μm . Furthermore, homogenous plate-like structures with a crystal width of 4.3 μm and a length of 700 μm are observable for 2.

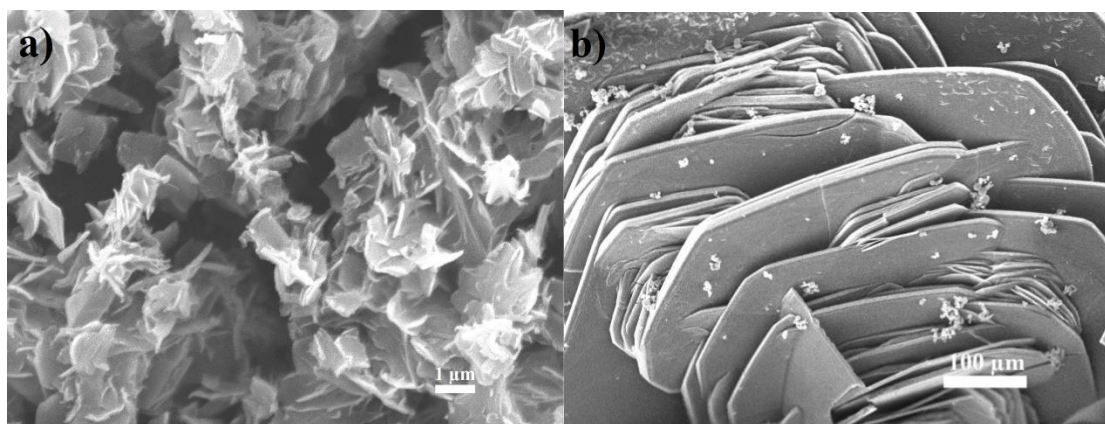


Fig. 1 SEM images of MOFs, 1(a) and 2(b)

Powder X-ray diffraction (PXRD) has been applied to study the phase purity and local geometry of the as-synthesized samples **1** and **2**, as presented in Figure 2a. As shown, the prominent peaks appear around 5° (2θ), 4.2 and 4.8 for compound **1** (Figure 2a), and 10° (2θ), 10.9 (Figure 2a) for compound **2** specifically, determining the formation of highly crystalline material that correlates with MOF crystal structure[24, 29].

Figure 2b demonstrates the thermogravimetric analyses (TGA) assessing the thermal stability of the MOFs **1** and **2**. For MOF **1** (Figure 2b), the first weight loss occurs in a temperature range between 120 - 240°C (5.37%) and can be assigned to the loss of lattice water molecules and DMF molecules. The second weight loss takes place between 260 - 480°C (40.72%), likely owing to the loss of the remaining DMF molecules. The weight loss for MOF **2** (Figure 2b) exhibits three steps at temperatures ranging between 20 - 120°C (20.33%), 160 - 260°C (10.76%), and 300 - 460°C (36.34%), which may be attributed to the loss of lattice water and DMF molecules from the samples' surface and cavities. However, both frameworks are stable up to at least 300°C .

The FT-IR spectra of $\text{H}_2\text{L}^+\text{Cl}^-$, 4, 4'-bipyridine, **1**, and **2** are presented in Figure 2c. The spectrum of $\text{H}_2\text{L}^+\text{Cl}^-$ demonstrates a strong absorption band at 1702 cm^{-1} attributed to the $\nu(\text{C}=\text{O})$ stretching vibration of uncoordinated carboxylate acid group, $-\text{COOH}$. This shift is a consequence of the deprotonation of the carboxyl groups present in the imidazolium ligands and occurs due to the coordination of the carboxylate group with the metal. Furthermore, the band at 3268 cm^{-1} assigned to the $\nu(\text{N-H})$ stretching vibration due to the interaction between 4,4'-bipyridine and water (present in the metal sources) is not present in the spectrum of **1** and **2**, proofing the coordination of 4,4'-bipyridine to metal centers in the frameworks. These results verify that the reaction of mixed 1,3-bis(4-carboxyphenyl)imidazolium chloride and 4,4'-bipyridine with $\text{Ni}(\text{NO}_3)_2 \cdot 6\text{H}_2\text{O}$ or $\text{Zn}(\text{NO}_3)_2 \cdot 6\text{H}_2\text{O}$ led to the coordination of both ligands with Ni(II) and/or Zn(II) to form the desired MOF structures, **1** and **2**, respectively. The sharp band at 1367 cm^{-1} for **1** and 1362 cm^{-1} for **2** represents the presence of NO_3^- anions present in the MOF cavities.

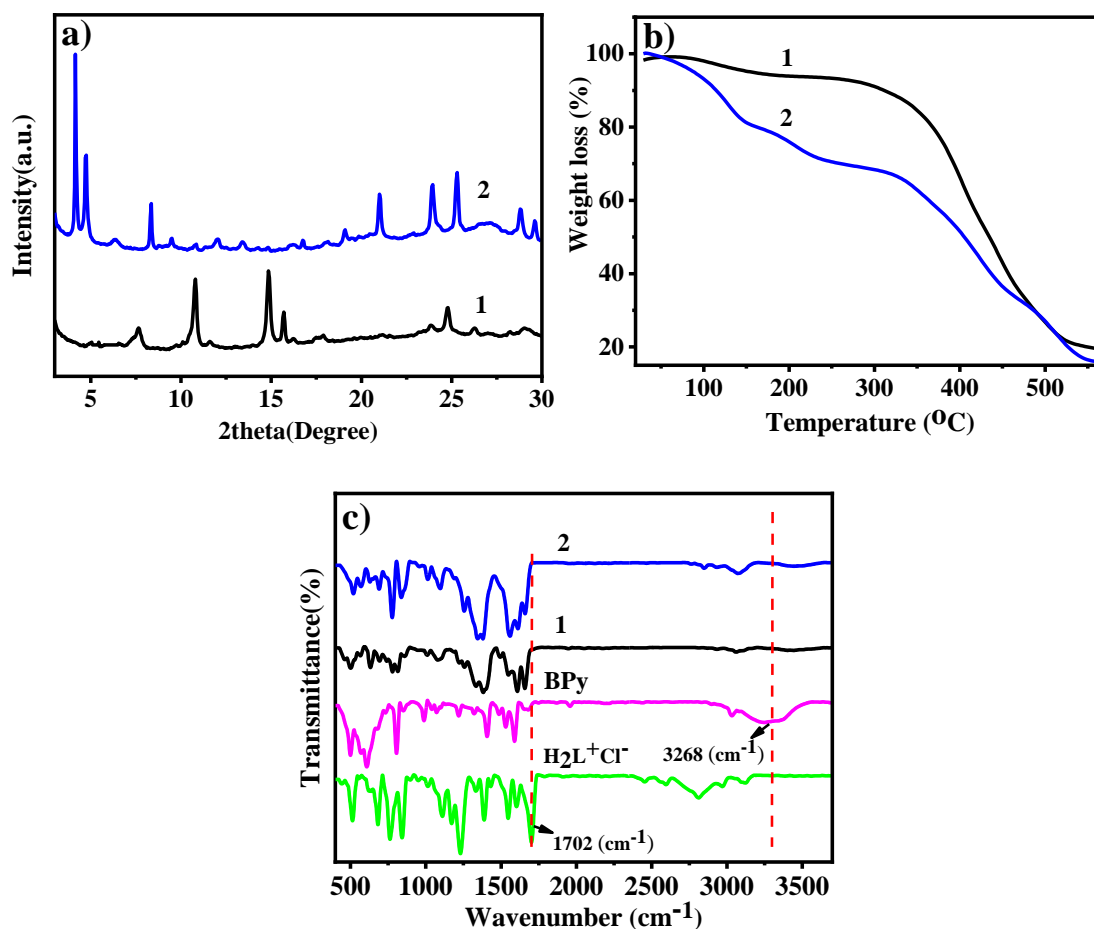


Fig. 2 a) PXRD pattern of compound 1 and 2. b) Thermal stability of the frameworks 1 and 2. c) FTIR spectra of $\text{H}_2\text{L}^+\text{Cl}^-$, 4, 4'-bipyridine, 1 and 2, illustrating the coordination of the ligands with the metals with formation of the frameworks.

The porosity properties of the two as-synthesized MOFs were analyzed by Brunauer–Emmett–Teller (BET) method, as presented in table S1. The calculated surface areas of MOF 1 and 2 were 24.67 and 20.80 cm^2/g , respectively. Such small surface areas are assigned to the high degree of interpenetration of these kinds of MOFs, resulting from the bending structure of the azolium ligand[29].

2.2 CO_2 and CH_4 adsorption of compound 1 and 2

As described previously, a cationic MOF can be created due to the positively charged aromatic azolium component of the ligands. Considering this particular characteristic, which is useful for gas separation, the superior absorptivity of two different gases in terms of polarity was investigated. Hence, CO_2 and CH_4 isotherms were determined for the two as-synthesized frameworks, 1 and 2, as presented in Figure 3. The adsorption of CO_2 is considerably higher than the methane uptake for both Ni (1) and Zn (2) azolium-bipyridine based MOFs. Rapid CO_2 adsorption in the initial stage implies a privileged interaction between CO_2 molecules (high quadrupole moment and polarizability) and the positively charged host frameworks. Methane molecules interact less with the frameworks and, as a result, demonstrate less adsorption[4, 5]. The CO_2 adsorption capacity of these MOFs 1, 2 are compared with those of MOFs containing different azolium ligands as a linker in their structure

(Table S2). As was reported, these azolium based MOFs exhibit a small CO₂ adsorption capacity as a result of the bent structure of the azolium ligands.

The lower CH₄ uptake can be attributed to its non-(quadru-)polar characteristic[4]. On the contrary, the high quadrupole moment ($-13.4 \times 10^{-40} \text{ C m}^2$) and polarizability ($26.3 \times 10^{-25} \text{ cm}^3$) of CO₂ resulted in superior adsorption [30, 31] owing to the strong electrostatic interactions with the positively charged frameworks[5]. Notably, the strong interaction between CO₂ molecules and the frameworks makes the desorption of CO₂ molecules sluggish[32, 33]. Accordingly, the disparity in the gases' polar structure and the MOFs' cationic characteristics is the essential explanation of the superior sorption of CO₂ over CH₄.

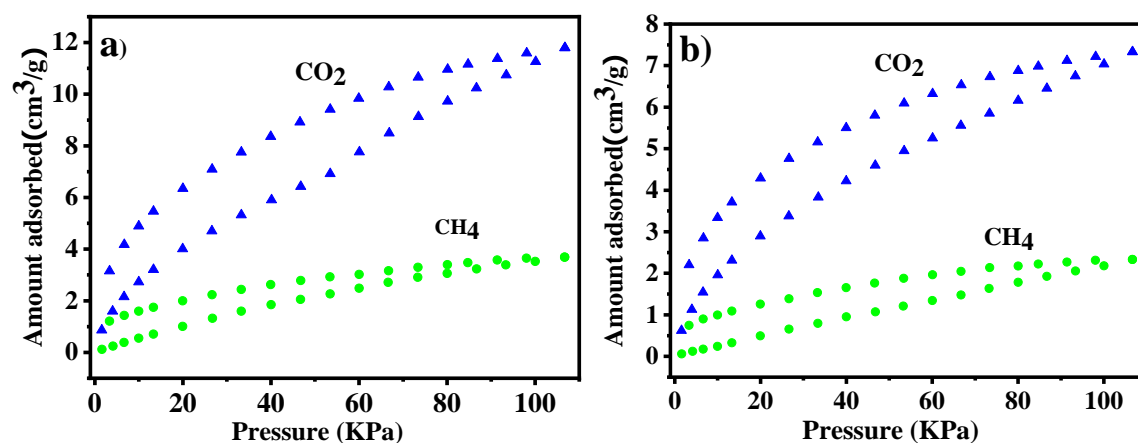


Fig. 3 The CO₂ and CH₄ isotherms of 1(a) and 2(b).

The Ideal Adsorption Solution Theory (IAST) proposed by Myers and Praunitz[34] was further employed to predict the CO₂/CH₄ adsorption selectivity, thereby evaluating the extent of the interaction of azolium frameworks with these gases. Figures 4a and 4b illustrate the IAST selectivity of CO₂ over CH₄, which confirms remarkably favorable interactions between 1 and 2 with CO₂ at low pressure. The high selectivity is due to the synergistic effects of the charged azolium struts that create an electropositive environment within the MOFs and the unsaturated metal sites in the framework structure. Therefore, CH₄ with lower quadrupole moment and polarizability interacts less with both MOFs, unveiling the potential applications of these azolium frameworks for gas separation. Notably, the higher CO₂/CH₄ selectivity of 2 than 1 is in agreement with the little higher anionic dye adsorption capacities of 2 compared to 1. Overall, the IAST selectivity results further confirm the electrostatic interactions between these azolium frameworks and the adsorbates. In conclusion, combining the sorption and IAST selectivity results, the electronic environment of 1 and 2 plays a decisive role in the selective sorption of CO₂ over CH₄.

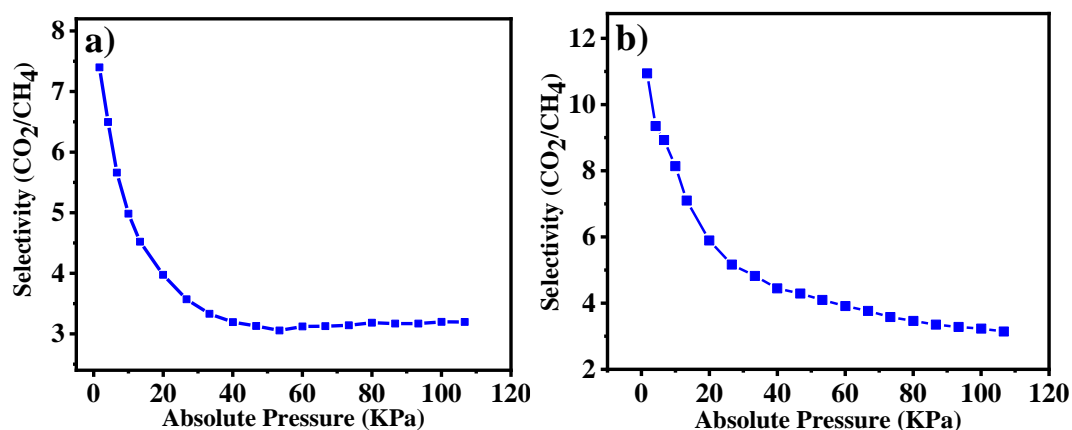


Fig. 4 IAST adsorption selectivity of CO₂ over CH₄ for 50/50 binary mixture at 273 K for 1(a) and 2(b).

2.3 Dye adsorption of compound 1 and 2

Besides, the charged nature of these two MOFs, **1** and **2**, motivated us to apply these compounds to assess their capacity for dye adsorption. Consequently, we arranged an experiment for dye adsorption employing **1** and **2** and several dyes, including cationic and anionic dyes in an aqueous solution. Accordingly, six dyes: electrically positively charged Nile Blue A (NBA), Rhodamine Blue (RhB), and Methylene Blue (MB) and negatively charged Orange II sodium salt (OS), Congo Red (CR), and Methyl Orange (MO) were selected as the models for dye-uptake experiments. UV-Vis spectroscopy was utilized to study the adsorption behaviors of compounds **1**, **2** toward these dyes. Figure 5 and Figure S2 illustrate the various performances of the two compounds **1**, **2** in an aqueous solution of anionic and cationic dyes, respectively.

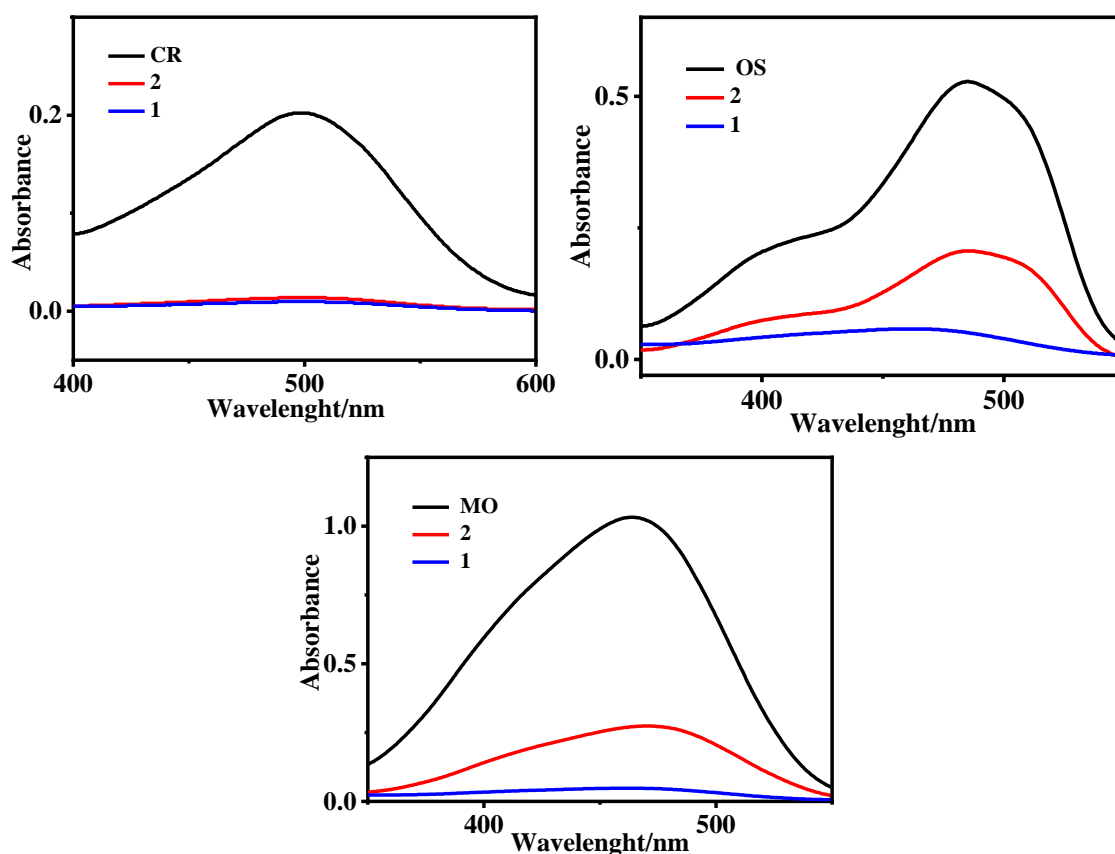


Fig. 5 The uptake of Anionic dyes (CR, OS, MO) over compounds **1**, **2** in an aqueous medium.

Figure 5 illustrates that frameworks **1** and **2** adsorb up to 95 % of CR, 75.93 % and 79.65 % of OS, and 75.04 % and 81.08% of MO, respectively. Furthermore, Figure S2 depicts the percentage adsorption capacity of MOFs **1** and **2** for MB (23.7 % and 19.5 %), RhB (52.9 % and 41.4 %), and NBA (23.97 % and 13.29 %). The abovementioned results demonstrate that **1** and **2** exhibit an excellent capacity to absorb anionic dyes. Figures 5 and S2 reveal that both MOFs, **1** and **2**, reveal higher adsorption for anionic dyes than for the cationic counterparts due to their positive charge present in the frameworks deriving from the azolium linker[18]. Hence, for compounds **1** and **2**, a higher affinity for adsorption of MO, CR, and OS (anionic dyes) was observed compared to those obtained for MB, RhB, and NBA (cationic dyes). In this experiment, neutral dyes were not employed due to their insolubility in aqueous media. In the following, the comparison of the maximum adsorption of CR over MOFs **1**, **2** with those of other adsorbents is reported in table S3, demonstrating the advantage of applying azolium based MOFs for this purpose. The two azolium based MOFs **1** and **2** displayed comparable adsorption capacity, suggesting the effectiveness of these materials for removing anionic dyes from contaminated aqueous medium. Worth mentioning is that considering the small pore volume of these two MOFs and dye molecules' size, dye molecules cannot get through these materials' pores.

2.4 Characterization of the post-modified MOF(1-Pd)

High-resolution powder X-ray diffraction (PXRD) was applied to examine the phase purity and crystallinity of post-modified **1**; see Figure 6a. Fortunately, the crystal structure of the as-synthesized MOF **1** remained the same after post-modification, as determined by the matching PXRD spectra of the as-synthesized MOF (**1**) and the post-modified MOF (**1-Pd**). To evaluate the thermal stability of **1-Pd**, thermogravimetric analysis was conducted on **1-Pd**, applying a heating rate of 10 °C/min. As

illustrated in Figure 6b, a weight loss is observed between 240-310 °C, which could be assigned to the loss of DMF molecules remaining in the framework after the post-modification[27]. The total collapse of the structure occurs at 400 °C signifying that **1** could retain its thermal stability after the post-synthetic modification, Figure 6b.

The FT-IR analysis of **1-Pd** is presented in Figure 6c, which is completely matched with **1** (figure 1c). This matching affirms that the structure of **1** did not change during PSM.

The surface morphology of PSM was studied using field-emission scanning electron microscopy (FE-SEM). The FE-SEM image of **1-Pd** shows no significant changes in surface morphology compared with that of the as-synthesized MOF. Thus, the framework did not undergo any deformation after PSM.

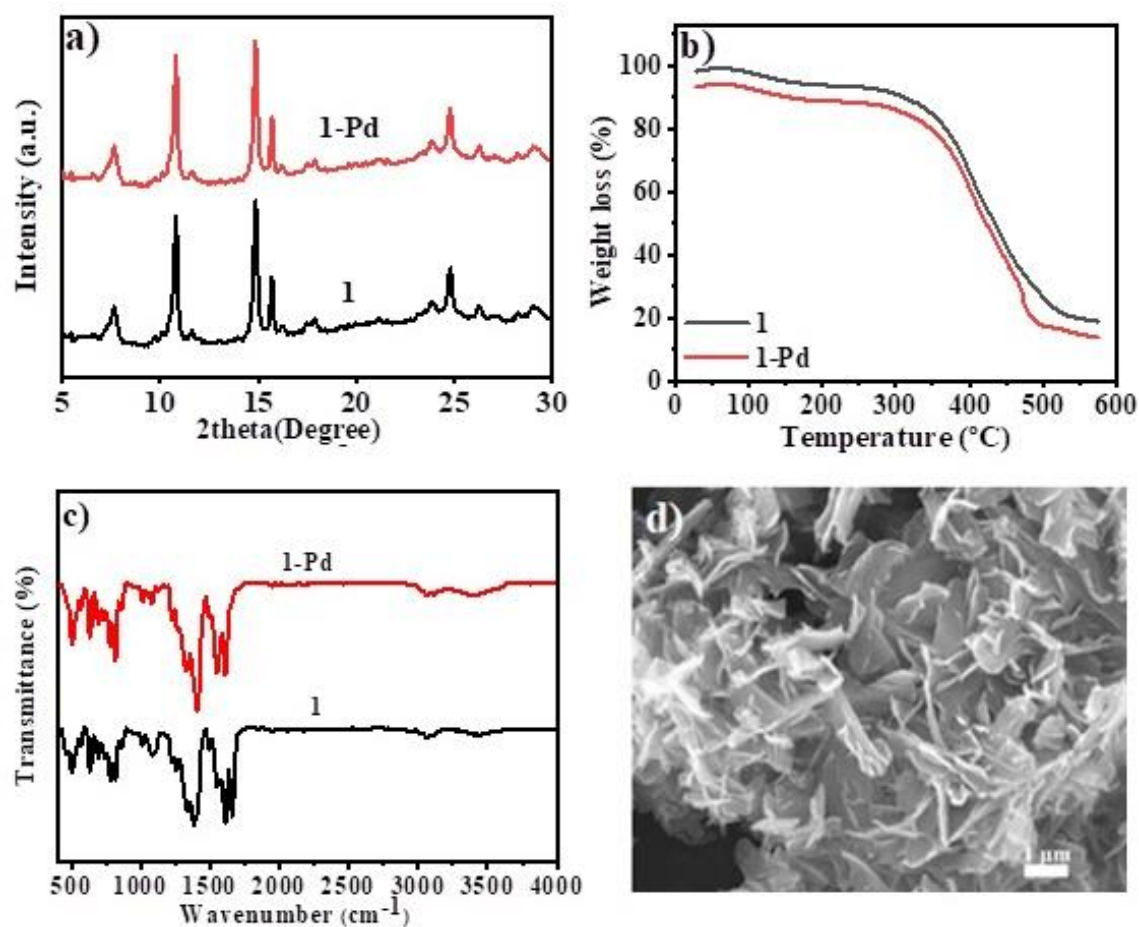


Fig. 6 a) PXRD pattern for post-synthetic modified MOF **1-Pd**. b) TG of MOF **1-Pd**, illustrating the thermal stability of this MOF. c) FT-IR spectrum of MOF **1-Pd**. d) SEM image of the post-modified MOF, **1-Pd**.

High-resolution transmission electron microscopy (HR-TEM) was used to characterize the surface morphology of **1-Pd** after post-modification with Pd and to examine the level of possible aggregation of Pd after post-synthetic modification (Figure 7). Examination of the TEM image of **1-Pd** (Figure 7b) revealed the existence of high density and homogeneous distribution of black areas with a maximum diameter of 10 nm on the surface of the frameworks (as some are identified with a yellow circle). Comparing figures 7a and 7b,c demonstrates no black areas in the TEM image of the as-synthesized MOF **1**, which confirms the Pd coordination to the ligand in the structure of **1** (Figure 7b, c). Besides, the ICP-MS result revealed the quantitative amount of Pd(II) as 9.65%.

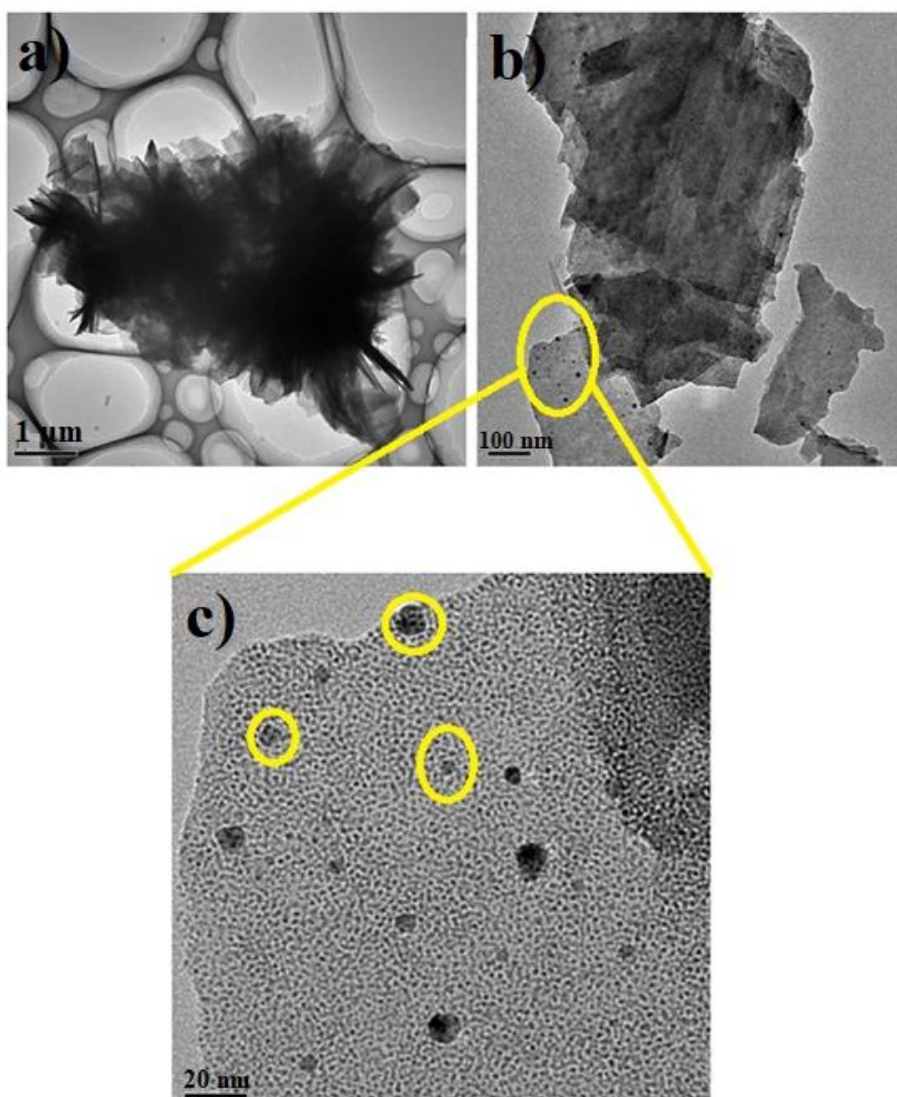


Fig. 7 a) TEM image of MOF **1**, b) HR-TEM image of **1-Pd**, c) Pd is coordinated to ligand in black areas of MOF **1** (yellow circles).

The binding energies of Pd and Ni of (**1-Pd**) were studied by X-ray photoelectron spectroscopy (XPS). The general survey scan of the XPS analysis (figure 8b) demonstrates the presence of Ni, Pd, N, C, and O in the modified framework. The binding energy of the N 1s in the imidazolium moieties appears at 400.2 eV[35]. Figure 8b illustrates the best curve-fit of the Pd XPS data. The binding energies arising at 336.72 and 342 eV are related to Pd 3d_{5/2} and 3d_{3/2}, respectively. These binding energies are typical for Pd (II)[36, 37] and are in excellent agreement with the values reported for Pd(II)-NHC complexes[29, 38]. Accordingly, this result confirms that Pd is in the +2 oxidation state. The characteristic binding energies for Ni (II) are presented as a doublet (Ni 2p_{1/2} - 2p_{3/2}) on 872.35 and 854.7 eV, respectively, (Figure 8c)[39]. No peaks of Ni metal, around 853 eV, were observed and the peak at 860.28 eV is a satellite peak.

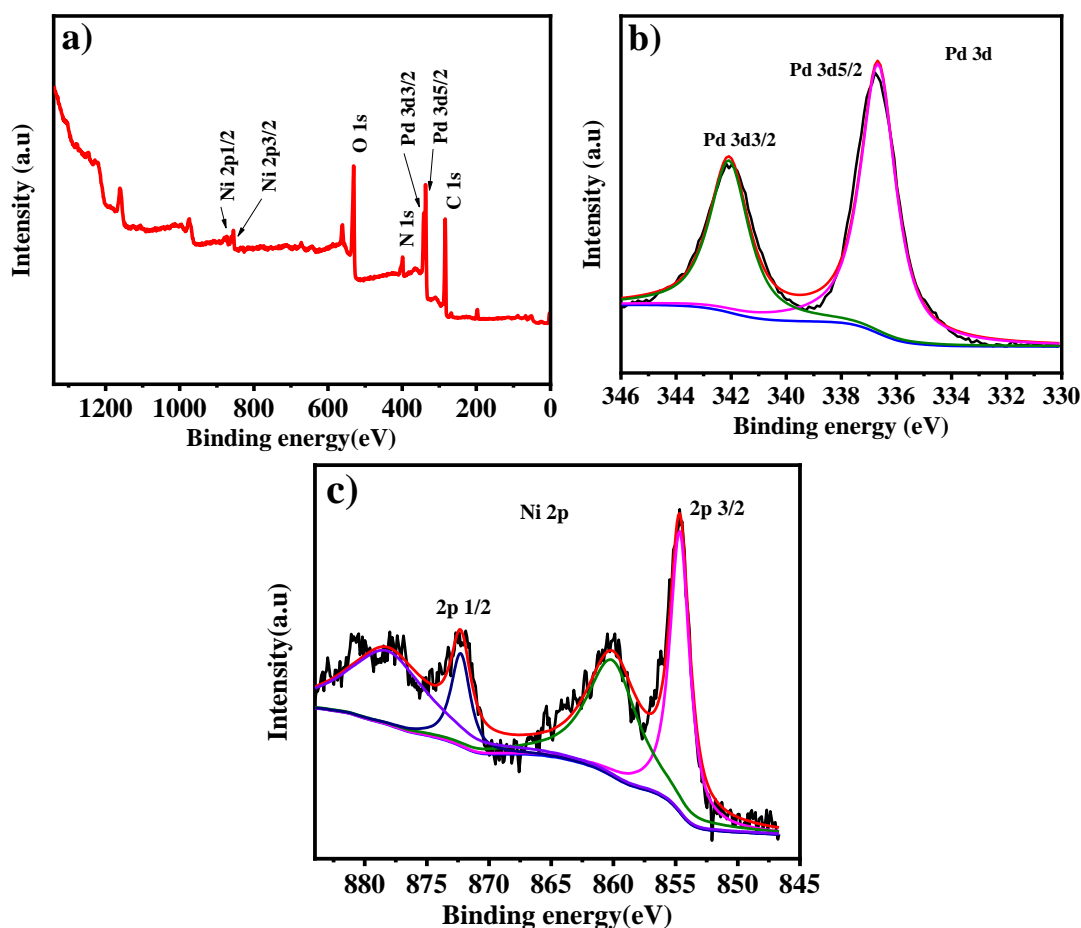


Fig. 8 a) XPS survey of the post-modified MOF **1-Pd**, demonstrating the presence of Pd, Ni, C, O, and N, b) High-resolution spectrum of Pd 3d, c) High-resolution spectrum of Ni 2p.

2.5 Catalytic activity of MOF **1-Pd** in Sonogashira and Suzuki C-C coupling reaction:

The significant Pd-catalyzed coupling reaction, known as the Sonogashira cross-coupling reaction, was investigated to assess the catalytic performance of **1-Pd**. The representative data are summarized in Table 1. This coupling reaction was carried out using substituted aryl halide, substituted phenylacetylene, K_2CO_3 , **1-Pd** in DMF at $100^\circ C$ under air atmosphere for 12 h to produce the desired products as presented in Table 1.

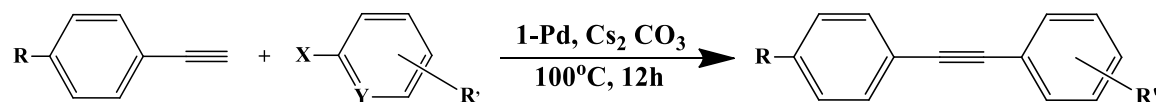
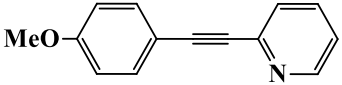
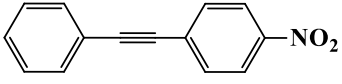
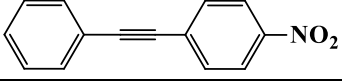


Table 1. Sonogashira cross-coupling reaction of various substrates with **1-Pd**

Entry	R	X	Y	R'	Product	Yield(%) ^b
1	H	Br	H	4-NO ₂		90.3
2	4C(CH ₃) ₃	Br	H	4-NO ₂		88.2
3	4-OCH ₃	Br	H	4-NO ₂		95.51

4	4-OCH ₃	Br	N	H		89.53
5	H	Br	H	4-NO ₂		45.6 ^c
6	H	Br	H	4-NO ₂		88.43 ^d

^aReaction conditions: aryl halide (0.92 mmol), phenylacetylene (1.1 mmol), Cs₂CO₃ (1.84 mmol), catalyst (15 mg) in 6 mL DMF heated at 100°C under air atmosphere for 12 h. ^bIsolated yield, ^cCatalyzed by Pd(OAc)₂, ^dafter 3 runs.

Under these reaction conditions, the catalyst (compound **1**) generates a higher yield of products (Table 1, entry 3) when phenylacetylene bears a *para*-substituted electron-withdrawing group compared with phenylacetylene compounds bearing a *para*-substituted electron-donating group (Table 1, entry 2). The electron-withdrawing group attached to the phenylacetylene generates a more acidic acetylene proton resulting in an easier cleavage during the coupling reaction. As a reference, we further applied Pd(OAc)₂ as a catalyst; however, the obtained yield was significantly lower (Table 1, entry 5). As illustrated in Table 1, entry 6, the catalytic performance did not exhibit any significant product yield changes after the third catalytic run. The ¹H-NMR analyses of the products are displayed in Figure S4-7 of supporting information. MOF **1-Pd** was analyzed after the third reaction cycle using PXRD and SEM. From the XRD spectrum and the SEM images (Figure S3), no variations can be observed of this MOF after three reaction cycles.

Additionally, the catalytic activity of **1-Pd** was evaluated for the Suzuki-Miyaura coupling reaction of phenylboronic acid phenyl halides. This coupling reaction was implemented with phenylboronic acid, substituted aryl halide, K₂CO₃, and **1-Pd** in ethanol at 60 °C under an air atmosphere for 6 h to produce the related products presented in Table 2. Under the given reaction conditions, excellent yields are obtained by applying aryl halide bearing *para*-substituted electron-withdrawing groups (Table 2, entries 2, 3) in comparison with aryl halide without any substituent (Table 2, entry 1). An electron-withdrawing group makes the cleavage of halides much easier. Entry 4 in Table 2 demonstrates that the yield of the product catalyzed by **1-Pd** catalyst remains unchanged after three runs for the Suzuki-Miyaura. Notably, the product yield catalyzed by Pd(OAc)₂ is far less than the yield obtained using **1-Pd** as catalyst (Table 2, entry 5). The ¹H-NMR analyses of the products are displayed in Figures S7-9 of supporting information. Furthermore, this MOFs' (**1-Pd**) catalytic activity in C-C coupling was compared with some other MOFs which contain Pd (II) anchored to either bipyridine or NHC linkers in their structures. As shown in table S4, this **1-Pd** MOF has an excellent catalytic activity comparable to its counterparts.

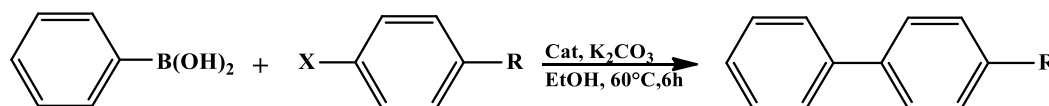
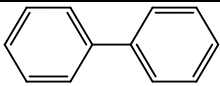
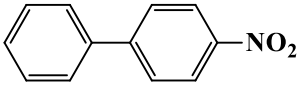
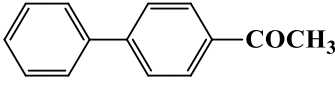
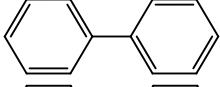
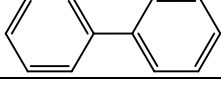


Table 2. Suzuki-Miyaura coupling reactions of phenylboronic acid and phenyl halides catalyzed by **1-Pd**

Entry	X	R	Product	Yield (%) ^a
-------	---	---	---------	------------------------

1	Br	H		89.2
2	Br	NO ₂		94
3	Br	COCH ₃		92
4	Br	H		87.8 ^b
5	Br	H		23.45 ^c

Reaction conditions: phenylboronic acid (1.2 mmol), Aryl halide (1.0 mmol), K₂CO₃ (2.0 mmol), **1-Pd** (15 mg), EtOH (4 mL) at 60 °C under air atmosphere. ^aIsolated yield, ^b third cycle, ^cCatalyzed by Pd(OAc)₂.

4. Materials and Methods

All initial chemicals and solvents were purchased from commercial sources and directly applied as received.

The azolium ligand, 1,3-bis(4-carboxyphenyl)imidazolium chloride (H₂L⁺Cl⁻), was synthesized in two steps according to the literature [27].

4.1 Ligand Synthesis

4.1.1 Synthesis of *N, N'*-Bis(4-carboxyphenyl)ethylenediimine (L_A)

4-aminobenzoic acid (10 g, 72.92 mmol, 2.0 equiv) was dissolved in 30 mL dry methanol. Then, formic acid (four drops) was added, followed by dropwise addition of 40% W/W aqueous glyoxal solution (4.18 mL, 36.46 mmol, 1.0 equiv), stirring at ambient temperature for 24 h. The resultant solid white product was collected by filtration, washed with cold methanol, and dried in air named compound L_A.

4.1.2 Synthesis of 1,3-Bis(4-carboxyphenyl)imidazolium chloride (H₂L⁺Cl⁻)

Under an argon atmosphere, compound L_A (5 g, 16.89 mmol) was dissolved in anhydrous THF (30 mL) followed by addition of a solution of paraformaldehyde (635 mg, 21.16 mmol, and 1.25 equiv) in 12 M HCl (2.1 mL, 25.33 mmol, 1.5 equiv). Next, dioxane (4 mL) at 0 °C was added, followed by stirring for 4 h at room temperature. The product was collected through filtration (Scheme 1), washed with Et₂O, and dried under vacuum.

4.2 MOF Synthesis

Compounds **1, 2** were synthesized as follows; A mixture of H₂L⁺Cl⁻ (23.78 mg, 0.069 mmol), 4, 4'-bipyridine (10.8 mg, 0.069 mmol), and Ni(NO₃)₂·6H₂O (81.1 mg, 0.279 mmol) or Zn(NO₃)₂·6H₂O (82.5 mg, 0.279 mmol) in 3 mL of DMF was added in a Teflon-lined stainless steel autoclave and heated at 90 °C for 48 h (Scheme 1). Then, the product was cooled to room temperature at a rate of 10 °C/h. Finally, the product was collected through filtration and washed with the pre-dried DMF.

4.3 Gas Adsorption Experiments

The sorption isotherm of CO₂ and Methane using activated MOFs **1** and **2** were explored at relative pressure p/p_0 of 1 at STP. Sample activation involved the solvent exchange with EtOH, followed by vacuum drying at 100 °C for 12 h.

4.4 A General Procedure for Dye Adsorption Experiments

To assess the dye adsorption capability of compounds **1**, **2**, 10 mL of an aqueous dye solution (100 mg/L), 10 mg of the as-synthesized framework were added in a 20 mL reaction vessel. The mixture was stirred at room temperature for 24 h. After that, the solid part was collected through centrifuging, and the liquid part was diluted to 1/10 of the stock solution and analyzed by UV-Vis absorption spectroscopy. The efficiency of the dye adsorption frameworks was calculated based on the percentage of degradation D% as follows:

$$D\% = (A_0 - A) / (A_0) \times 100\%$$

Where A_0 and A shows the absorbance of the liquid sample before and after degradation, respectively.

4.5 Post-synthetic Modification of MOF 1

NiMOF (MOF **1**) was post-modified with palladium acetate according to the literature[24, 28]. In a typical procedure, THF solution (20 mL), Pd(OAc)₂ (30 mg, 0.13 mmol), and **1** (100.0 mg) were introduced in a 50 mL two-necked round bottom flask followed by stirring at ambient temperature for 6 h and refluxing for 4 h under an inert N₂ atmosphere. The resultant light green-yellowish solid (**1-Pd**) was centrifuged, washed with THF, MeOH, and Et₂O, and dried in air.

4.6 A typical procedure for the Sonogashira C-C coupling reaction

Phenylacetylene (0.92 mmol), aryl halide (1.1 mmol), Cs₂CO₃ (1.84 mmol), **1-Pd** (15 mg), and DMF (6 mL) were introduced in a round-bottomed flask and stirred at room temperature under air atmosphere for 12 h. The solid was filtered and washed twice with DMF (3 mL) after being cooled to room temperature. The filtrate was collected, dried, and ethyl acetate (3×3 mL) was employed to extract the residue, and the related product was achieved by purification using silica gel chromatography (eluent: petroleum ether). Finally, the products were identified by ¹H-NMR.

4.7 A general procedure for the Suzuki-Miyaura cross-coupling reaction

A mixture of aryl halide (1.0 mmol), phenylboronic acid (1.2 mmol), K₂CO₃ (2 mmol), and **1-Pd** (15 mg) in 5 mL of ethanol was stirred for 6 h at 60 °C under air atmosphere in a 10 mL round-bottomed flask. The reaction mixture was cooled to room temperature, centrifuged, and extracted with ethanol. Next, the organic layer was dried over anhydrous Na₂SO₄ and concentrated in a vacuum. Chromatography on silica gel using hexane/ethyl acetate as eluent was used to give the isolated yield. The isolated yield was obtained based on aryl halide.

4.8 Recycling Test

To assess the catalyst's recyclability, the catalyst was separated through the centrifuge, washed with DMF, and dried at 100 °C under vacuum overnight after each run of the coupling reaction. After that, under the same reaction conditions, the catalyst was used again in the reaction. The product was subsequently isolated in the same way applied in the first run, and the catalyst was separated to be applied in the next cycle.

4.9 Characterization

Powder X-ray diffraction patterns (PXRD) were obtained on a Bruker D8 advanced diffractometer, applying Cu K α radiation within a 2 θ angle at ambient conditions. The materials' texture was recorded on a scanning electron microscope (SEM) from JEOL (JSM-5610LV, 0.5–35 kV). A Netzsch (STA449c/3/G) instrument was employed to achieve thermogravimetric analyses (TGA–DSC) at a heating rate of 10 °C/min under an inert atmosphere (N₂-flow). Tunnel electron microscopy (TEM) and high resolution-Tunnel electron microscopy (HR-TEM) analysis were carried out in a Philips CM20 microscope operated at 200 kV. ¹H-NMR spectra were obtained at 500 MHz, if not otherwise stated, using a Brüker 500 MHz NMR spectrometer referenced to tetramethylsilane (TMS). Fourier transform infrared (FT-IR) spectra were measured on a Perkin-Elmer Spectrum One spectrometer. UV–Vis spectrometry was recorded applying a UV-3600, Shimadzu, Japan. X-ray photoelectron spectroscopy (XPS) was applied to study the surface electronic state on a Perkin-Elmer PHI 5000C ESCA. C1s= 284.6 eV was used as a reference to calibrate all the binding energy values. The Pd contents were determined by inductively coupled plasma optical emission spectra (ICP, Varian VISTAMPX).

5. Conclusions

The two frameworks of **1** and **2** are synthesized by applying two ligands, 1,3-bis(4-carboxyphenyl)imidazolium chloride and 4,4'-bipyridine, and two metal salts of Zn and Ni, respectively. The positively charged aromatic azolium moieties create a cationic environment in the frameworks. In gas adsorption, it was demonstrated that these two frameworks have more affinity to adsorb CO₂ over methane. This phenomenon is attributed to the strong interaction between CO₂ molecules and the charged frameworks. As the CO₂ molecules are polar, they can be adsorbed by positively charged frameworks more than the non-polar methane.

Besides, in liquid phase adsorption, these charged frameworks prove proficient in removing anionic dyes from contaminated aqueous medium. In addition, in this examination, MOF (**1**) was post-modified with palladium on the carbene site of the azolium ligand to generate the catalyst **1-Pd**. The crystallinity and morphology of the MOF **1** remain after metallation. **1-Pd**, as a catalyst, demonstrated suitable activities in C-C coupling reactions such as Sonogashira and Suzuki-Miyaura reactions. The catalytic activity remains the same after three cycles of reaction. Overall, these mixed azolium-pyridine incorporated frameworks have potential applications for the separation of CO₂ from flue gases, for adsorptive removal of negatively charged organic contaminants, and as an efficient catalyst for C-C coupling reactions.

Supplementary Materials: the porosity properties, H-NMR data, the graphs of dye adsorption related to cationic dyes, and the PXRD and SEM image of 1-Pd after catalytic reaction can be found in supplementary materials.

Author Contributions: N.G, A.G.G. and F.V. devised the concept for the work and designed the experiments. N.G., C.I.E. and S.R. synthesized the materials, carried out the characterization and interpretations. N.G., C.I.E. and S.R. carried out catalysis and adsorption experiments. N.G. wrote the draft of the manuscript. A.G.G. and F.V. revised the manuscript. A.G.G. and F.V. supervised the whole work.

Funding: F.V. acknowledges the financial support from the State Key Laboratory of Advanced Technology for Materials Synthesis and Processing, Wuhan University of Technology.

Acknowledgments: The authors would like to acknowledge State Key Laboratory of Advanced Technology for Materials Synthesis and Processing, Wuhan University of Technology. S.R, A.G.G. and F.V. acknowledge and appreciate the support of the University of Guilan.

Conflicts of Interest: no conflict of interest is declared.

References

1. Grünkner, R.; Bon, V.; Müller, P.; Stoeck, U.; Krause, S.; Mueller, U.; Senkovska, I.; Kaskel, S. A new metal–organic framework with ultra-high surface area. *Chem. Commun* **2014**, *50* (26), 3450.
2. Deng, H.; Grunder, S.; Cordova, K. E.; Valente, C.; Furukawa, H.; Hmadeh, M.; Gándara, F.; Whalley, A. C.; Liu, Z.; Asahina, S. Large-pore apertures in a series of metal-organic frameworks. *science* **2012**, *336* (6084), 1018.
3. Lan, Y. Q.; Jiang, H. L.; Li, S. L.; Xu, Q. Mesoporous metal-organic frameworks with size-tunable cages: selective CO₂ uptake, encapsulation of Ln³⁺ cations for luminescence, and column-chromatographic dye separation. *Adv. Mater* **2011**, *23* (43), 5015.
4. Lee, J. Y.; Roberts, J. M.; Farha, O. K.; Sarjeant, A. A.; Scheidt, K. A.; Hupp, J. T. Synthesis and gas sorption properties of a metal-azolium framework (MAF) material. *Inorg. Chem* **2009**, *48* (21), 9971.
5. Sen, S.; Neogi, S.; Aijaz, A.; Xu, Q.; Bharadwaj, P. K. Construction of Non-Interpenetrated Charged Metal–Organic Frameworks with Doubly Pillared Layers: Pore Modification and Selective Gas Adsorption. *Inorg. Chem* **2014**, *53* (14), 7591.
6. Raghu, S.; Basha, C. A. Chemical or electrochemical techniques, followed by ion exchange, for recycle of textile dye wastewater. *J. Hazard. Mater* **2007**, *149* (2), 324.
7. Masoud, R.; Haroun, A.; El-Sayed, N. Dyeing of chrome tanned collagen modified by in situ grafting with 2-EHA and MAC. *J. App. Polym. Science* **2006**, *101* (1), 174.
8. LIU, J. Papermaking technology evolution: Its impact on wet-end retention. *PaperTechnol* **2005**, *46* (8), 31.
9. Turesky, R. J.; Freeman, J. P.; Holland, R. D.; Nestorick, D. M.; Miller, D. W.; Ratnasinghe, D. L.; Kadlubar, F. F. Identification of aminobiphenyl derivatives in commercial hair dyes. *Chem. Res. Toxicol* **2003**, *16* (9), 1162.
10. Esther, F.; Tibor, C.; Gyula, O. Removal of synthetic dyes from wastewaters: a review. *Environ. Int* **2004**, *30* (7), 953.
11. Yagub, M. T.; Sen, T. K.; Afroze, S.; Ang, H. M. Dye and its removal from aqueous solution by adsorption: a review. *Adv. Colloid Interface. Sci* **2014**, *209*, 172.
12. Attia, A. A.; Rashwan, W. E.; Khedr, S. A. Capacity of activated carbon in the removal of acid dyes subsequent to its thermal treatment. *Dyes Pigm* **2006**, *69* (3), 128.
13. Haque, E.; Lee, J. E.; Jang, I. T.; Hwang, Y. K.; Chang, J.-S.; Jegal, J.; Jhung, S. H. Adsorptive removal of methyl orange from aqueous solution with metal-organic frameworks, porous chromium-benzenedicarboxylates. *J. Hazard. Mater* **2010**, *181* (1-3), 535.
14. Haque, E.; Jun, J. W.; Jhung, S. H. Adsorptive removal of methyl orange and methylene blue from aqueous solution with a metal-organic framework material, iron terephthalate (MOF-235). *J. Hazard. Mater* **2011**, *185* (1), 507.
15. Yang, J.-M.; Yang, B.-C.; Zhang, Y.; Yang, R.-N.; Ji, S.-S.; Wang, Q.; Quan, S.; Zhang, R.-Z. Rapid adsorptive removal of cationic and anionic dyes from aqueous solution by a Ce (III)-doped Zr-based metal–organic framework. *MicroporMesopor Mat* **2020**, *292*, 109764.

16. Cui, Y.-Y.; Zhang, J.; Ren, L.-L.; Cheng, A.-L.; Gao, E.-Q. A functional anionic metal–organic framework for selective adsorption and separation of organic dyes. *Polyhedron* **2019**, *161*, 71.
17. Nickerl, G.; Notzon, A.; Heitbaum, M.; Senkovska, I.; Glorius, F.; Kaskel, S. Selective adsorption properties of cationic metal–organic frameworks based on imidazolic linker. *Cryst. Growth Des* **2012**, *13* (1), 198.
18. Ezugwu, C. I.; Asraf, M. A.; Li, X.; Liu, S.; Kao, C.-M.; Zhuiykov, S.; Verpoort, F. Selective and adsorptive removal of anionic dyes and CO₂ with azolium-based metal-organic frameworks. *J. Colloid Interface. Sci* **2018**, *519*, 214.
19. Ezugwu, C. I.; Asraf, M. A.; Li, X.; Liu, S.; Kao, C.-M.; Zhuiykov, S.; Verpoort, F. Cationic nickel metal-organic frameworks for adsorption of negatively charged dye molecules. *Data in brief* **2018**, *18*, 1952.
20. Chughtai, A. H.; Ahmad, N.; Younus, H. A.; Laypkov, A.; Verpoort, F. Metal-organic frameworks: versatile heterogeneous catalysts for efficient catalytic organic transformations. *Chem. Soc. Rev* **2015**, *44* (19), 6804.
21. Mousavi, B.; Chaemchuen, S.; Moosavi, B.; Luo, Z.; Gholampour, N.; Verpoort, F. Zeolitic imidazole framework-67 as an efficient heterogeneous catalyst for the conversion of CO₂ to cyclic carbonates. *New J. Chem* **2016**, *40* (6), 5170.
22. Gholampour, N.; Chaemchuen, S.; Hu, Z.-Y.; Mousavi, B.; Van Tendeloo, G.; Verpoort, F. Simultaneous creation of metal nanoparticles in metal organic frameworks via spray drying technique. *Chem. Eng. J.* **2017**, *322*, 702.
23. Oisaki, K.; Li, Q.; Furukawa, H.; Czaja, A. U.; Yaghi, O. M. A Metal– organic framework with covalently bound organometallic complexes. *J. Am. Chem. Soc* **2010**, *132* (27), 9262.
24. Ezugwu, C. I.; Mousavi, B.; Asraf, M. A.; Luo, Z.; Verpoort, F. Post-synthetic modified MOF for Sonogashira cross-coupling and Knoevenagel condensation reactions. *J. Catal* **2016**, *344*, 445.
25. Choudary, B. M.; Madhi, S.; Chowdari, N. S.; Kantam, M. L.; Sreedhar, B. Layered double hydroxide supported nanopalladium catalyst for Heck-, Suzuki-, Sonogashira-, and Stille-type coupling reactions of chloroarenes. *J. Am. Chem. Soc* **2002**, *124* (47), 14127.
26. Xue, L.; Lin, Z. Theoretical aspects of palladium-catalysed carbon–carbon cross-coupling reactions. *Chem. Soc. Rev* **2010**, *39* (5), 1692.
27. Sen, S.; Nair, N. N.; Yamada, T.; Kitagawa, H.; Bharadwaj, P. K. High proton conductivity by a metal–organic framework incorporating ZnO clusters with aligned imidazolium groups decorating the channels. *J. Am. Chem. Soc* **2012**, *134* (47), 19432.
28. Kong, G.-Q.; Xu, X.; Zou, C.; Wu, C.-D. Two metal–organic frameworks based on a double azolium derivative: post-modification and catalytic activity. *Chem. Commun* **2011**, *47* (39), 11005.
29. Ezugwu, C. I.; Mousavi, B.; Asrafa, M. A.; Mehta, A.; Vardhan, H.; Verpoort, F. An N-heterocyclic carbene based MOF catalyst for Sonogashira cross-coupling reaction. *Catal. Sci. Technol* **2016**, *6* (7), 2050.
30. Mason, J. A.; Sumida, K.; Herm, Z. R.; Krishna, R.; Long, J. R. Evaluating metal–organic frameworks for post-combustion carbon dioxide capture via temperature swing adsorption. *Energy Environ. Sci* **2011**, *4* (8), 3030.
31. Bourrelly, S.; Llewellyn, P. L.; Serre, C.; Millange, F.; Loiseau, T.; Férey, G. Different adsorption behaviors of methane and carbon dioxide in the isotopic nanoporous metal terephthalates MIL-53 and MIL-47. *Energy & Environmental Science* **2005**, *127* (39), 13519.

32. Cui, P.-P.; Zhao, Y.; Lv, G.-C.; Liu, Q.; Zhao, X.-L.; Lu, Y.; Sun, W.-Y. Synthesis, characterization and selective hysteretic sorption property of metal–organic frameworks with 3, 5-di (pyridine-4-yl) benzoate. *Cryst. Eng. Comm* **2014**, *16* (28), 6300.
33. Bhattacharya, B.; Saha, D.; Maity, D. K.; Dey, R.; Ghoshal, D. Syntheses, X-ray structures, gas adsorption and luminescent properties of three coordination polymers of Zn (II) dicarboxylates mixed with a linear, neutral, and rigid N, N'-donor ligand. *Cryst. Eng. Comm* **2014**, *16* (22), 4783.
34. Myers, A. L.; Prausnitz, J. M. Thermodynamics of mixed-gas adsorption. *AIChE Journal* **1965**, *11* (1), 121.
35. Kovač, B.; Ljubić, I.; Kivimäki, A.; Coreno, M.; Novak, I. The study of the electronic structure of some N-heterocyclic carbenes (NHCs) by variable energy photoelectron spectroscopy. *Phys. Chem. Chem. Phys* **2015**, *17* (16), 10656.
36. Bai, C.; Jian, S.; Yao, X.; Li, Y. Carbonylative Sonogashira coupling of terminal alkynes with aryl iodides under atmospheric pressure of CO using Pd (II)@ MOF as the catalyst. *Catal. Sci. Technol* **2014**, *4* (9), 3261.
37. Xu, S.; Song, K.; Li, T.; Tan, B. Palladium catalyst coordinated in knitting N-heterocyclic carbene porous polymers for efficient Suzuki–Miyaura coupling reactions. *J. Mater. Chem A* **2015**, *3* (3), 1272.
38. Liu, G.; Hou, M.; Wu, T.; Jiang, T.; Fan, H.; Yang, G.; Han, B. Pd (ii) immobilized on mesoporous silica by N-heterocyclic carbene ionic liquids and catalysis for hydrogenation. *Phys. Chem. Chem. Phys* **2011**, *13* (6), 2062.
39. Li, Z.; Dong, H.; Zhang, Y.; Li, J.; Li, Y. Enhanced removal of Ni (II) by nanoscale zero valent iron supported on Na-saturated bentonite. *J. Colloid Interface Sci* **2017**, *497*, 43.